NASA Technical Memorandum 83294

MODELING STIFFNESS LOSS IN BORON/ALUMINUM BELOW THE FATIGUE LIMIT

W. S. Johnson

March 1982

National Aeronautics and Space Administration

Langley Research Center
Hampton, Virginia 23665

LIST OF SYMBOLS

E^f	fiber elastic modulus, MPa
E^m	matrix elastic modulus, MPa
E^m_{eff}	effective modulus of the matrix in the loading direction, MPa
E_N	unloading elastic modulus at N number of cycles
E_o	initial elastic modulus of the first cycle (modulus of undamaged laminate), MPa
E_S	secant modulus
E_{SDS}	laminate modulus assuming damaged matrix material, MPa
R	stress ratio, S_{min}/S_{max}
S_{max}	maximum laminate stress, MPa
S_{min}	minimum laminate stress, MPa
S_{11}	laminate stress in the 0° fiber direction, MPa
S_{22}	laminate stress in the 90° fiber direction, MPa
Y	cyclic-hardened yield stress, corresponds to one-half the matrix fatigue limit for R = 0, MPa
$\Delta\varepsilon$	laminate strain range
$\Delta\varepsilon^m_{comp}$	compressive strain range of the matrix material in the loading direction
ΔS	laminate stress range, MPa
ΔS_{Sh}	stress range that causes no fatigue damage, MPa
σ^f	axial stress in the fiber in the loading direction
σ^m	axial stress in the matrix in the loading direction
σ^m_{sh}	stress in the matrix material in the loading direction when the matrix yields

ABSTRACT

Previous research has shown that boron/aluminum can develop significant internal matrix cracking when fatigued. These matrix cracks can result in a 40 percent secant modulus loss in some laminates even when fatigued below the fatigue limit. The present study shows that the same amount of fatigue damage will develop during stress or strain controlled tests. Stacking sequence has little influence on secant modulus loss. The secant modulus loss in unidirectional composites is small, whereas the losses are substantial in laminates containing off-axis plies. This paper presents a simple analysis that predicts unnotched laminate secant modulus loss due to fatigue. The analysis is based upon the elastic modulus and Poisson's ratio of the fiber and matrix, fiber volume fraction, fiber orientations, and the cyclic-hardened yield stress of the matrix material. Excellent agreement was achieved between model predictions and experimental results. With this model, designers can project the material stiffness loss for design load or strain levels and assess the feasibility of its use in stiffness critical parts.

INTRODUCTION

Metal matrix composites (MMC), in spite of their relatively high cost, have several inherent properties that make them attractive for structural applications; MMC have high stiffness-to-weight ratios, high strength-to-weight ratios, and better transverse strength, better operative temperature range, and environmental resistance than do competitive epoxy-resin-matrix composites. Many components are of continuous fiber-reinforced MMC, such as boron/aluminum (B/Al).

Previous research [1-3] has shown that boron/aluminum can develop significant internal matrix cracking even when cycled below the fatigue limit. This results in laminate modulus loss. In quasi-isotropic laminates, matrix cracks reduce stiffness as much as 40 percent. Because most MMC structural components are expected to be stiffness critical, even a small drop in component stiffness may render the part useless or cause failure of the structure.

This paper builds upon the data base developed in References [1-3,9] by adding results for three additional laminates. These additional tests are conducted under both strain and load control. References [1-3,9] dealt with fatigue mechanisms while this paper produces information that is more design applicable. The damage model analysis presented in Reference [1] is modified and expanded to predict the laminate secant modulus after approximately 500,000 fatigue cycles (when the laminate is in a saturation damage state). The analysis needs only the elastic modulus and Poisson's ratio of the fiber and matrix, fiber volume fraction, fiber orientations, and the cyclic-hardened yield stress of the matrix material. With this analysis, designers can project the material stiffness loss for design load or strain levels and assess the feasibility of its use in stiffness critical parts.

The secant modulus is predicted for eight different laminates and compared to experimental test results. The tests were conducted at numerous stress and strain levels below the fatigue limit. Test and predictive results are discussed.

EXPERIMENTAL PROCEDURE

The material tested was unnotched boron-aluminum composites with a 6061 aluminum matrix and 0.14 mm diameter boron fibers. Table 1 presents

material properties for the boron and aluminum constituents and Table 2 shows the eight laminates that were tested. Notice that five laminates ($[0]_8$, $[0/90]_{2S}$, $[90/0]_{2S}$, $[0/\pm45/90/0/\pm45/\overline{90}]_S$ and $[0/\pm45/90]_S$) are from previous references and three laminates ($[0/\pm45]_S$, $[0_2/\pm45]_S$, and $[\pm45/0_2]_S$) are new. The laminate specimen widths are shown in Table 2. All specimens were annealed such that the 6061 aluminum matrix was in the annealed condition before testing. All specimens were fatigue loaded at 10 cycles per second except when the stress-strain response of the material was recorded on an x-y plotter. The stress-strain data were taken under quasi-static condition periodically during test life. The strain was measured with a 25.4 mm gage-length extensometer. All specimens tested for this study were cycled at constant amplitude stress or strain levels below their fatigue limit. The stress ratio, R, was constant for each test presented. Different specimens were tested at R ranging from 0.0 to 0.5.

To obtain the data generated in Reference [3], fatigue tests were conducted at a constant amplitude stress range until failure or to two million cycles. The secant modulus of approximately the 500,000th cycle was obtained from recorded stress-strain data. Therefore, each tested specimen provided one data point for the 500,000th cycle response. The tests conducted in the present study (laminates $[0_2/\pm45]_S$, $[\pm45/0_2]_S$, and $[0/\pm45]_S$) were somewhat different. To generate more data per specimen, tests were conducted at a constant stress or strain level for 500,000 cycles (time enough for a saturation damage state to develop) and then the stress-strain response was recorded. The stress or strain range was then increased to a new desired level, and another 500,000 cycles applied. The resulting stress-strain response was recorded. This process was repeated up to as many as five

different stress or strain levels per specimen. Fatigue damage at each level depends only on the applied stress range and therefore is not influenced by the prior cycling at lower stress ranges [1].

BACKGROUND

If fatigue damage is to be avoided in general, and low cycle fatigue failures in particular, the cyclic loading must produce only elastic strains in the constituents. Even so, local plastic straining can be permitted in the composite during the first few load cycles, provided that the composite "shakes down" during these few cycles. The shakedown state is reached if the matrix cyclically hardens to a cyclic yield stress Y such that, subsequently, only elastic deformation occurs under load cycles. The shakedown limit for the composite containing 0° fibers is considerably below the composite's fatigue limit. Previous tests have shown that the matrix fatigue limit coincides with the stable cyclic yield stress for annealed aluminum [3,4,5] and [5]. The value of Y is 70.38 MPa for annealed 6061 aluminum [2,3].

The shakedown stress range for a unidirectionally loaded laminate can be found by using laminate theory to determine the yield surfaces for individual plies in the laminate. Figure 1 shows an example of a $[0/\pm45/90]_S$ layup under biaxial inplane stresses S_{11} and S_{22}. Each ply has its own elliptical yield surface, constructed analytically from the ply matrix stresses and the von Mises yield condition. The overall yield surface of the laminate is an internal envelope of the yield surfaces of individual plies. The shakedown stress range, ΔS_{Sh}, is the width of the overall yield surface in the S_{11} direction of uniaxial loading applied in this experimental program.

The value of ΔS_{Sh} can be easily calculated with computer program AGLPLY [6]. More details of this procedure can be found in References [3,7].

When a specimen was cycled above its shakedown range, matrix cracks were observed [3]. Figure 2 shows a micrograph of cracks in a 45° ply matrix. These matrix cracks reduce the effective tensile modulus of the matrix. The cracks tend to open and close under remotely applied cyclic loads. This matrix cracking and the subsequent crack opening and closing results in a bilinear response as will be explained later in the paper, but may be observed from experimental stress-strain responses as shown in Figure 3 for the 500,000th cycle. The amount of damage (matrix cracking) can be inferred from the changes in elastic unloading modulus, E_N, as described in References [1-3]. Stress-strain data were taken at intervals during the fatigue cycling to record the drop in laminate modulus as a function of the number of cycles. The damage was expressed in terms of its effect on E_N normalized by E_0. An example of the fatigue damage accumulation as a function of number of applied cycles and stress level is presented in Figure 4 for a $[0/\pm45/90/0/\pm45/\overline{90}]_S$ laminate. Most damage occurred in the first 500,000 cycles. Notice that each specimen appears to reach a stabilized value of E_N/E_0, herein referred to as a "saturation damage state" (SDS). After the saturation damage state is reached, the laminate will neither accumulate more damage nor fail under the present loading condition.

Returning to Figure 3, the cyclic stress-strain curve for the fourth cycle results from elastic and plastic deformation and has a secant modulus, E_S, of 10.82×10^4 MPa. For the same specimen, the 500,000th cyclic stress-strain curve has a very different shape with an associated secant modulus of 8.88×10^4 MPa. The shape change of the stress-strain curve and the drop in

secant modulus (almost 22 percent) is attributed primarily to matrix cracking. In contrast, hardening of the matrix material [2,3] usually caused the secant modulus to increase after some initial cycling. Notice that the fourth cycle in Figure 3 has a secant modulus much less than the elastic modulus (Table 2) just due to plasticity. If the laminate was cycled at or below the shakedown range, the matrix would harden such that the secant modulus would be approximately equal to the elastic modulus. To confirm that the decrease in elastic unloading modulus and secant modulus observed during fatigue cycle was caused by matrix cracking and not fiber breakage, the aluminum matrix was gradually etched in a 30 percent HCℓ solution in distilled water. Fiber failure was detected only in specimens tested at stresses near the fatigue limit. However, substantial laminate modulus changes were detected for specimens stressed well below this level. Specimens that sustained modulus loss had long matrix cracks that grew parallel to the fibers in the off-axis layers of the laminate. Some cracking perpendicular to the loading direction has been observed in the matrix of the 0° plies [8,9]. (Notice in Figure 1 that the 45° and 90° plies yield at a lower laminate stress than do the 0° plies; therefore, the matrix in the off-axis plies would be expected to undergo more plastic deformation which, in turn, would lead to more fatigue cracking than in the 0° plies. Indeed, the off-axis plies did have more cracks.) The individual cracks did not extend into adjacent plies that had different ply orientation. No delamination was discovered between the plies, as is commonly reported for polymer matrix composites. Therefore, practically all of the observed elastic unloading modulus decrease was caused by cracks in the matrix, since such cracks were the only observed damage of consequence.

DAMAGE MODEL

A version of this damage model was first presented in Reference [1,3]. The present model is quite similar except that the bounds on the matrix stress range, $\Delta\sigma^m$, are modified. Whereas the previous model was intended to calculate only laminate unloading elastic modulus, the present model is extended to calculate the secant modulus, E_s.

A simple analysis is developed to relate the decrease in laminate secant modulus caused by matrix damage. The model starts with the matrix cycling plastically. As cracks develop due to plastic cycling, the effective modulus is reduced for the portion of the matrix cycle that is in tension. The model presents simple equations to approximate the effective matrix modulus due to the cracking at an assumed cyclic strain range. The program AGLPLY is used to calculate the laminate response with the effective modulus of the fatigued matrix. Thus the bilinear response illustrated in Figure 3 is computed. The secant modulus is calculated from the bilinear response.

Figure 5 illustrates this behavior in terms of the applied laminate stress and the corresponding axial stresses in the matrix and 0° fibers. The dashed lines in Figure 5 represent the initial loading response. Accordingly, the first load cycle causes the matrix and 0° fiber stresses to follow the dashed loops. The laminate has an ideally elastic-plastic matrix (for illustration of the model and simplicity of presentation) and is subjected to a constant cyclic stress range, ΔS. The dashed loops are for the same condition represented in Figure 2 in the fourth cycle. σ^m_{Sh} is assumed to be the axial stress in the matrix material in the loading direction at the shakedown stress limit, ΔS_{Sh}, (the matrix is yielded at this point by a combination of axial and shear stresses). Assuming the matrix yields at the

same value in tension and compression, σ^m_{Sh} equals half of the laminate's shakedown strain range, $\Delta S_{Sh}/E_o$, times the matrix tensile modulus, E^m.

$$\sigma^m_{Sh} = \frac{\Delta S_{Sh}}{2E_o} \cdot E^m \qquad (1)$$

The ΔS_{Sh} in this equation is the shakedown stress range, E_o is the undamaged laminate's elastic modulus in the loading direction, and E^m is the undamaged matrix's elastic modulus. (σ^m_{Sh} is approximately equal to Y for unidirection composites. The axial matrix stresses at yielding was assumed to be Y and $-Y$ in the previous model [1].) With subsequent cycling, the cyclic plasticity causes matrix cracks to initiate and grow, effectively decreasing the matrix tensile modulus until a saturation damage state is reached. The dashed loops in Figure 5 narrow to zero-width loops, shown as solid lines, which represent the saturation damage state. These solid lines correspond to the laminate cyclic stress-strain response illustrated in Figure 3 for the 500,000th cycle. The saturation damage state develops when the matrix cracking causes the load to transfer to the 0° fibers, thus relieving the matrix from undergoing additional damaging plastic deformation.

The drop in matrix modulus in the load direction due to fatigue damage will now be determined using Figure 6. The strain in the matrix and laminate is plotted versus the matrix stress, σ^m, and laminate stress, S, respectively. The damage state has an associated cyclic strain range, $\Delta\varepsilon$. If this cyclic strain range is assumed, an effective tensile modulus E^m_{eff} of the matrix material can be estimated. This assumes thatthe same SDS will be reached by either stress or strain control. Note that E^m_{eff} is the modulus in the loading (0° fiber) direction. The compressive strain range of the matrix, $\Delta\varepsilon^m_{comp}$, was approximated by

$$\Delta\varepsilon^{m}_{comp} = \frac{\Delta S_{Sh}}{2E_o} \tag{2}$$

The effective tensile modulus of the matrix material can now be approximated by dividing σ^{m}_{Sh} by the cyclic strain minus the compressive portion.

$$E^{m}_{eff} = \frac{\sigma^{m}_{Sh}}{\Delta\varepsilon - \Delta\varepsilon^{m}_{comp}} \tag{3}$$

The E^{m}_{eff} is used as the matrix modulus in lamination theory (using the computer program AGLPLY [6]) to calculate the unloading elastic modulus of the composite in its saturation damage state, E_{SDS}, (at approximately 500,000 cycles). The shear modulus of the matrix is also reduced within ANGPLY based on E^{m}_{eff} and Poisson's ratio. All the fibers were assumed to be intact, the matrix damage was assumed to be characterized by the laminate's lower modulus, E^{m}_{eff}. Although such a formulation implicitly assumes that the matrix modulus is reduced isotropically, the reduction really is orthotropic. However, interest is in the laminate modulus in the primary loading direction only, and the assumption should not introduce excessive error.

Returning to Figure 6, we now know the modulus for each of the two linear segments, as well as the strain ranges. Therefore, the overall laminate stress range, ΔS, can be calculated as follows:

$$\Delta S = (\Delta\varepsilon^{m}_{comp})E_o + (\Delta\varepsilon - \Delta\varepsilon^{m}_{comp})E_{SDS}. \tag{4}$$

Equation (4) was rewritten using Equation (2).

$$\Delta S = E_{SDS}\,\Delta\varepsilon + \tfrac{1}{2}\,\Delta S_{Sh}(1 - E_{SDS}/E_o) \quad \text{for} \quad \Delta S > \Delta S_{Sh}$$

$$= E_o\,\Delta\varepsilon \quad \text{for} \quad \Delta S \leq \Delta S_{Sh}. \qquad (5)$$

The values of ΔS_{Sh}, E_o, and E_{SDS} came from AGLPLY. Equation (4) applies for either stress or strain control cycling. By selecting a number of different strain range values, $\Delta\varepsilon$, the corresponding laminate stress range, ΔS, can be calculated and plotted versus $\Delta\varepsilon$. The laminate secant modulus is

$$E_S = \Delta S/\Delta\varepsilon. \qquad (6)$$

RESULTS AND DISCUSSIONS

The predicted cyclic stress-strain response after 500,000 cycles and its associated secant modulus is presented in this section and compared with measured experimental results. The predictions are shown as solid lines (see Figure 7 as an example). For reference a dashed line representing the undamaged elastic modulus of the laminate is shown. The secant modulus scale can be read in two ways. First, by entering on the ΔS axis, crossing to the solid prediction line and down to the secant modulus scale; this would give the secant modulus of a laminate after 500,000 cycles at a given stress range. Secondly, one could simply drop from the cyclic strain scale directly to the secant modulus scale to assess the secant modulus after 500,000 cycles at a given strain range. Notice that the secant modulus scale is nonlinear. Also notice that the secant modulus scale ends on the left at the shakedown

limit; the secant modulus is equal to E_o below the shakedown limit. The experimental data were generated at stress ratios, R, between 0.0 and 0.5. Since all the data show little scatter, this confirms that the damage developed in the matrix is a function of stress range, ΔS, and not of R (or mean stress) [3].

Figures 7 through 12 present the experimental and analytical correlation in order of elastic modulus, highest to lowest.

Figure 9 and 10 presents data for the $[0_2/\pm45]_S$ and $[0/\pm45]_S$ laminates, respectively. These tests are significant because they were conducted under both stress and strain control. The experimental data indicate that the same damage state is reached whether the stress is held constant and the strain increases or the strain is held constant and the stress decreases. This material behavior allows one to assume a constant strain range to calculate fatigue damage for strain or stress control tests in the presented analysis.

Figure 8 and 11 include data points representing the initial cyclic response of the laminate (e.g., the fourth cycle in Figure 2). These data illustrate the secant modulus loss due to matrix yielding. The initial cyclic stress-strain responses are reasonably close to the predicted response after 500,000 cycles, however, as shown in Figure 3, the reason, or mechanism for the secant modulus loss is different.

Figures 8 and 9 show that stacking sequence has very little effect on the secant modulus, E_S, in $[0/90]_{2S}$ - $[90/0]_{2S}$, and $[0_2/\pm45]_S$ - $[\pm45/0_2]_S$ laminates, respectively. Previous research [1] showed that stacking sequence may have an effect on the degradation of the elastic unloading modulus, E_N, in particular, near the shakedown limit.

In general, the predictions fit the experimental data very well. The data fell slightly above the predictions in some cases and slightly below in others. Some of this scatter may be attributed to deviation of the fiber volume fraction from what was assumed. Also, the annealing treatment of the aluminum matrix may have varied from one laminate to another. It is also acknowledged that the assumption of isotropically decreasing the modulus of the matrix due to cracking may affect the predictive results for various laminates differently. In any case, the present model does a very good job of representing the extent of accumulated fatigue damage in the saturation damage state and predicting the observed material response.

The experimental data fit the predictions quite well, even though the individual data points were generated at different stress ratios. This confirms observations [3] that the matrix damage is a function of stress range and not mean stress.

The resulting secant modulus after 500,000 cyles is significantly below the elastic modulus for all of the tested laminates, except the $[0]_8$ laminate. If compared at a cyclic strain range of 0.004, the $[0]_8$ laminate retained approximately 95 percent of the original elastic modulus. The other laminates retained about 60 to 70 percent of their original moduli. These differences between the often calculated elastic modulus and the resulting secant modulus must be addressed by the designers of stiffness critical parts. Certainly the unidirectional laminate may still retain the desired stiffness, but laminates with off-axis plies must be scrutinized as to their design load levels and stiffness requirements.

SUMMARY

A simple model has been presented that will accurately predict the secant modulus loss, under fatigue loading, of boron/aluminum laminated composites. The model requires only knowledge about the fiber and matrix moduli and Poisson's ratio, fiber volume fraction, layup orientation, and the cyclic hardened yield strength for annealed materials (the fatigue limit of the matrix material). These properties, in conjunction with lamination theory and von Misses yield criterion are sufficient to predict modulus changes.

Since the assumptions are not restricted to boron fibers and no empirical constants are used, the author feels that this model can be applied to other continuous fiber reinforced metal matrix composite systems, particularly those with the matrix in the near annealed condition.

The experimental data indicated that the same degree of damage can be reached from either strain or stress control testing; this verifies a basic assumption in the model. The experimental data further indicated that laminate stacking sequence did not have a large influence on secant modulus drop. The presented results indicate that laminates with off-axis plies may result in secant moduli that are about 25 to 40 percent below the elastic moduli after fatigue cycling.

Hopefully, this model for metal matrix composites will help designers more fully understand these materials and their limitations. It is further intended to help the designers avoid the pitfalls that are caused by generating S-N fatigue data alone, without regard to the behavior of the material below the fatigue limit where the data in this paper were generated.

REFERENCES

[1] Johnson, W. S., "Mechanisms of Fatigue Damage in Boron/Aluminum Composites," NASA TM-81926, National Aeronautics and Space Administration, Washington, DC, Dec. 1980. (Also Damage in Composite Materials, ASTM STP 775, 1982.)

[2] Dvorak, G. J. and Johnson, W. S., "Fatigue of Metal Matrix Composites," International Journal of Fracture, Vol. 16, No. 6, Dec. 1980, pp. 585-607.

[3] Johnson, W. S., "Characterization of Fatigue Damage Mechanisms in Continuous Fiber Reinforced Metal Matrix Composites," Ph.D. thesis, Duke University, Dec. 1979.

[4] VanHorn, K. R., ed., Aluminum, Vol. 1, American Society for Metals, 1967, p. 183.

[5] Weng, Ming T., "Some Aspects of Fatigue Relative to Cyclic Yield Stress," International Journal of Fatigue, Vol. 3, No. 3, Oct. 1981, pp. 187-193.

[6] Bahei-El-Din, Y. A., "Plastic Analysis of Metal-Matrix Composite Laminates," Ph.D. thesis, Duke University, July 1979.

[7] Dvorak, G. J. and Bahei-El-Din, Y. A., "Plasticity of Composite Laminates," Proceedings of Research Workshop on Mechanics of Composite Materials, Duke University, Oct. 1978.

[8] White, M. K. and Wright, M. A., "The Fatigue Properties of Cross-Plied Boron 6061 Aluminum," Journal of Materials Science, Vol. 14, 1979, pp. 653-662.

[9] Dvorak, G. J. and Johnson, W. S., "Fatigue Mechanisms in Metal Matrix Composite Laminates," 1981 Advances in Aerospace Structures and Materials, ASME AD-01, 1981, pp. 21-34.

[10] Mayfield, Jerry, "New Fibers Developed for Composites," Aviation Week and Space Technology, Jan. 8, 1979, pp. 35-41.

[11] DiCarlo, J. A., "Mechanical and Physical Properties of Modern Boron Fibers," NASA TM-73882, National Aeronautics and Space Administration, Washington, DC, Apr. 1978.

TABLE 1.- COMPOSITE CONSTITUENTS MECHANICAL PROPERTIES

	Boron fiber [10,11] 0.142 mm diameter	6061 aluminum
Elastic modulus (GPa)	400	72.5
Poisson's ratio	0.13	0.33

TABLE 2.- DIMENSIONS AND PROPERTIES OF BORON/ALUMINUM LAMINATES

Laminate	V_F	Width mm	Thickness mm	Calculated	
				E_o, GPa MPa	ΔS_{Sh}, MPa
$[0]_8$*	0.45	12.70	1.47	220.0	459
$[0/90]_{2S}$*	0.50	12.70	1.37	184.4	220
$[90/0]_{2S}$*	0.50	12.70	1.37	184.4	220
$[0_2/\pm45]_S$	0.44	18.38	1.49	170.0	216
$[\pm45/0_2]_S$	0.44	18.38	1.49	170.2	216
$[0/\pm45]_S$	0.45	18.38	1.11	157.0	195
$[0/\pm45/90/0/\pm45/\overline{90}]_S$*	0.45	12.70	2.64	151.3	192
$[0/\pm45/90]_S$*	0.33	12.70	1.60	126.5	185

*Reference [3]

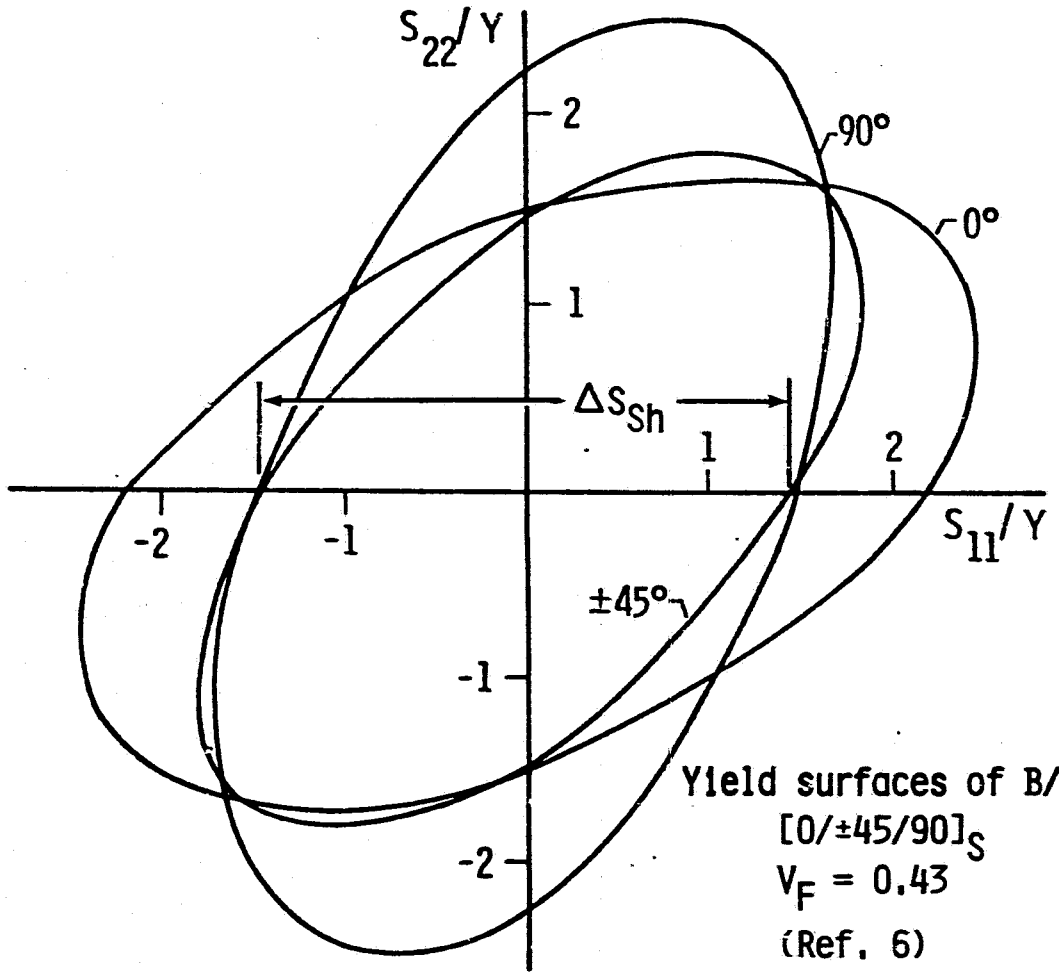

Figure 1.- Yield surfaces for plies of a B/Al laminate. The S_{11} direction coincides with 0° fiber direction.

ORIGINAL PAGE
BLACK AND WHITE PHOTOGRAPH

Figure 2.- Cracks in the +45° lamina matrix material at saturation damage state.

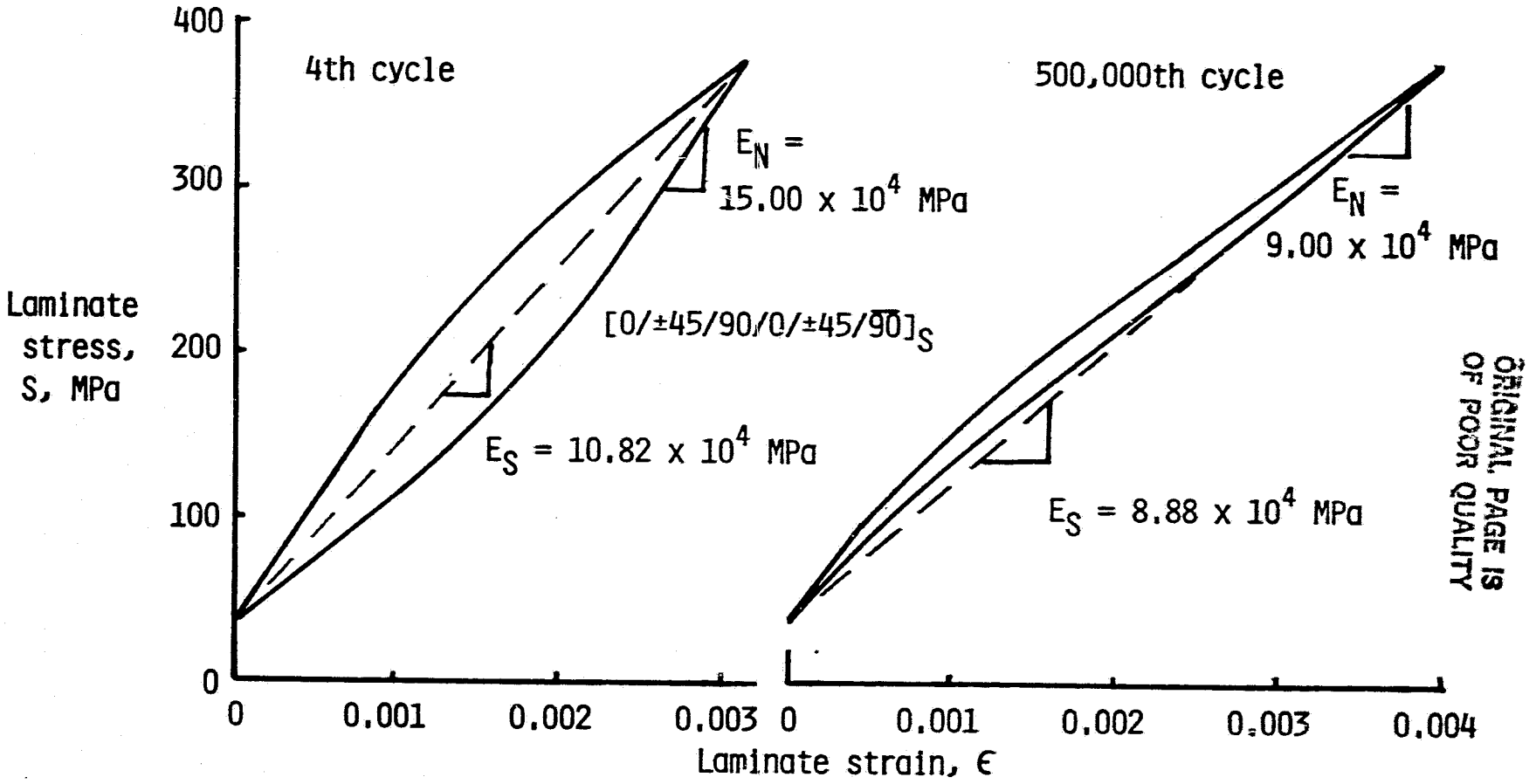

Figure 3.- Observed moduli in 4th cycle due to plasticity and observed moduli in 500,000th cycle due to matrix cracking.

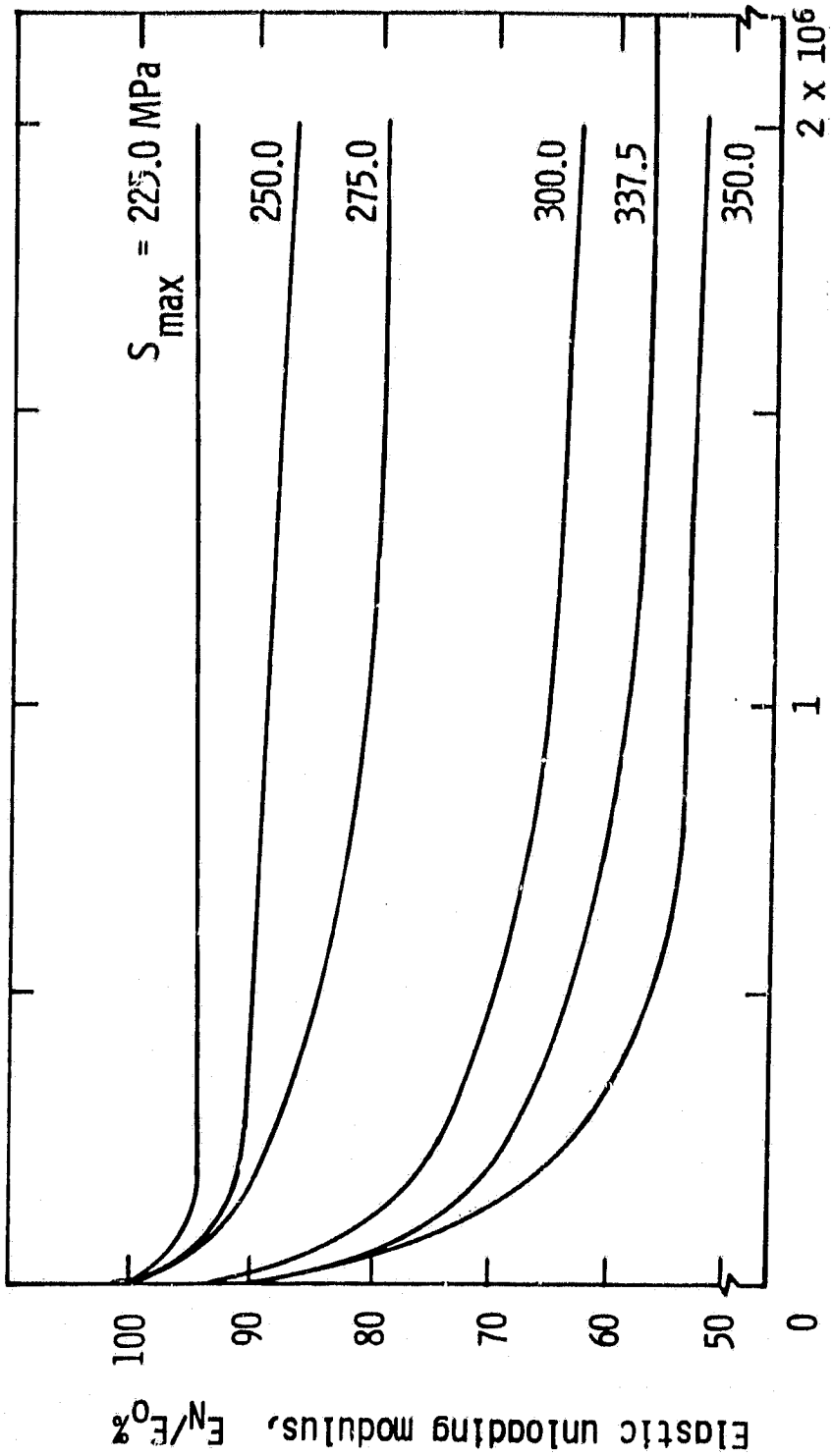

Figure 4.- Change in elastic unloading modulus of $[0/\pm45/90/0/\pm45/90]_S$. Specimens tested at different values of S_{max} at R = 0.1.

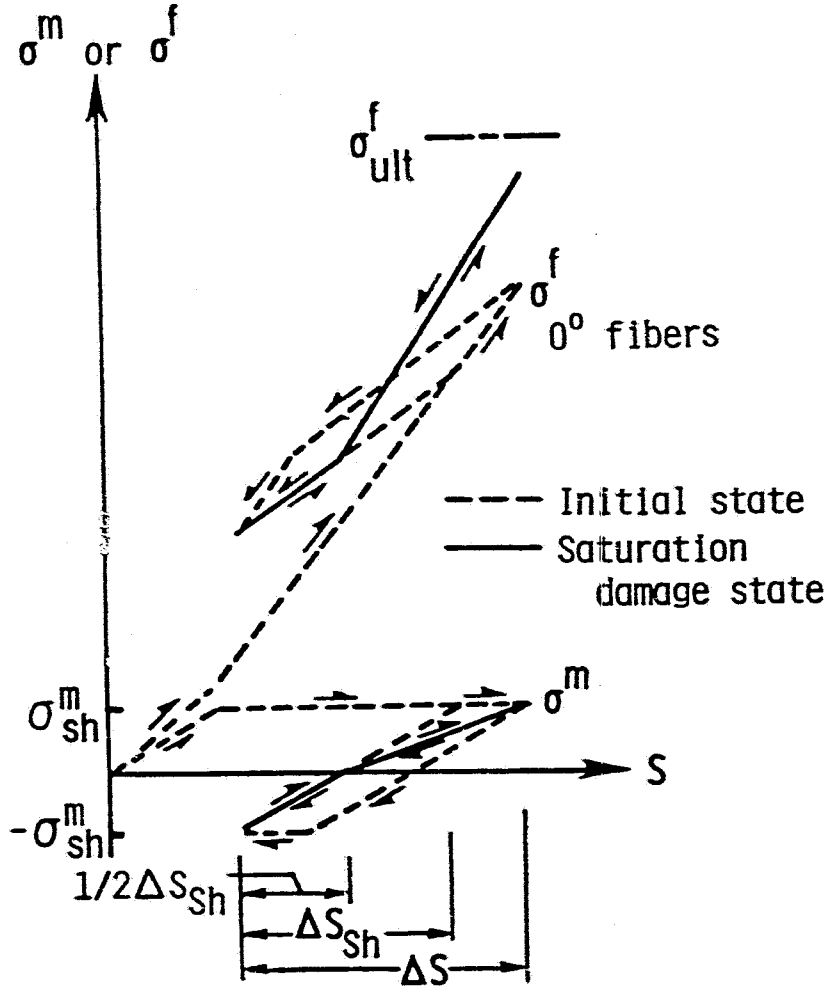

Figure 5.- Decreasing tensile matrix response and increasing 0° fiber stress as the laminate attains a saturation damage state.

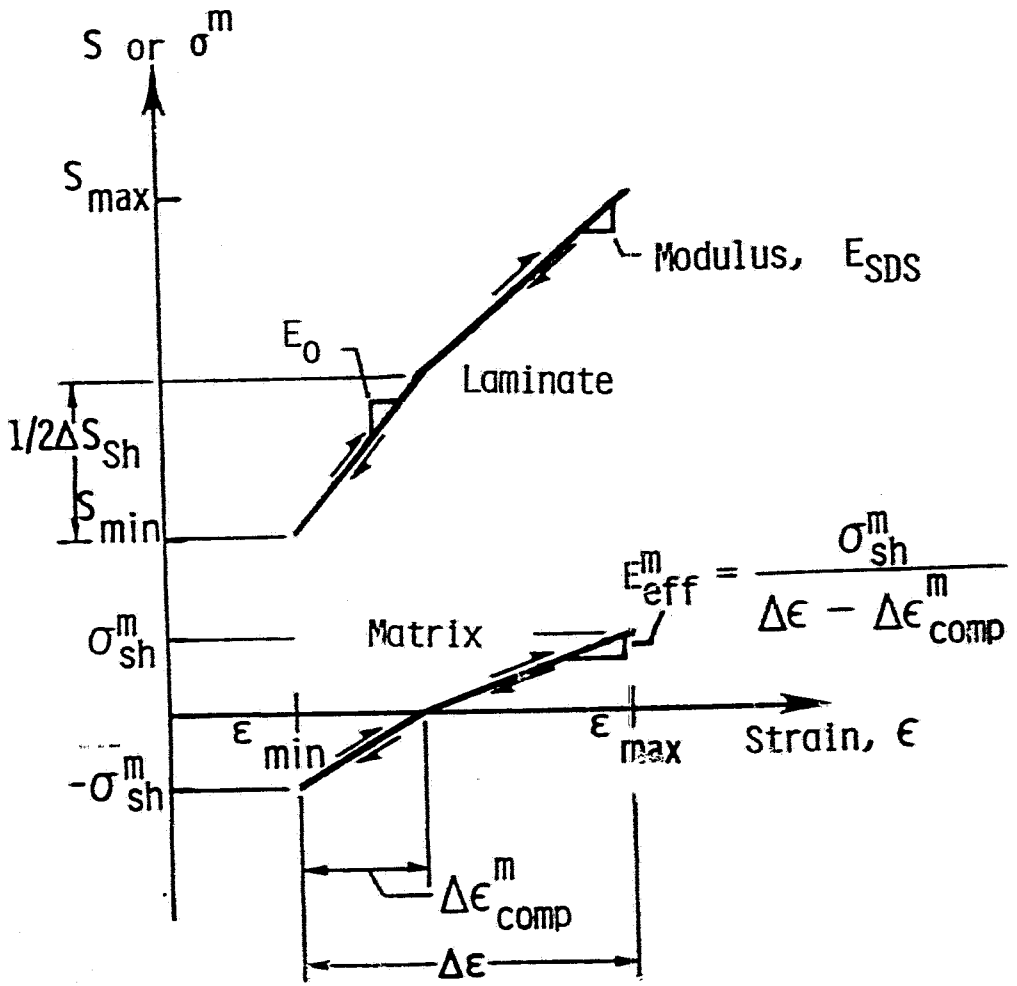

Figure 6.- Composite laminate and matrix stress-strain response for a saturation damage state.

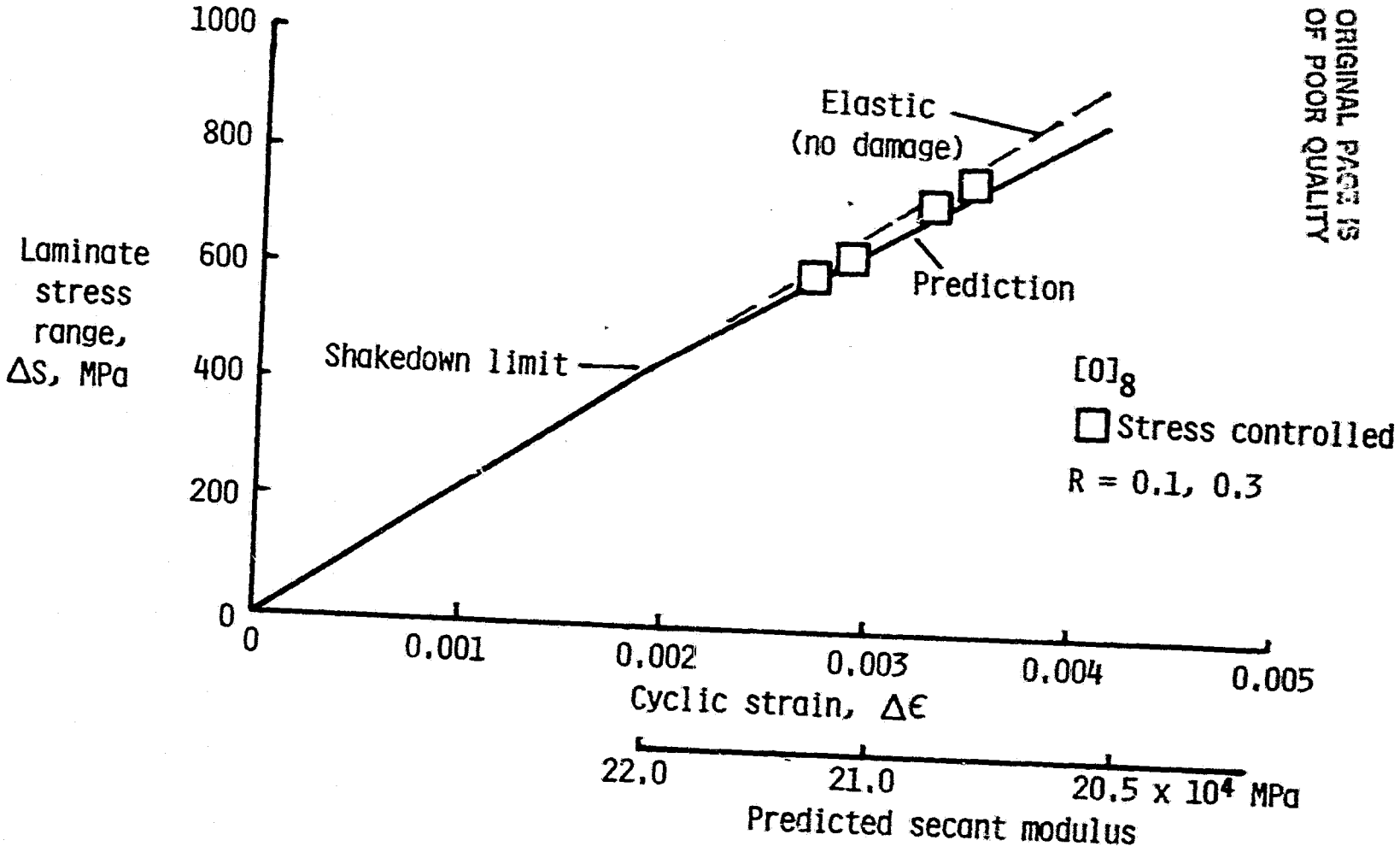

Figure 7.- Correlation of experimental and model predictions for $[0]_8$ laminate after 500,000 fatigue cycles.

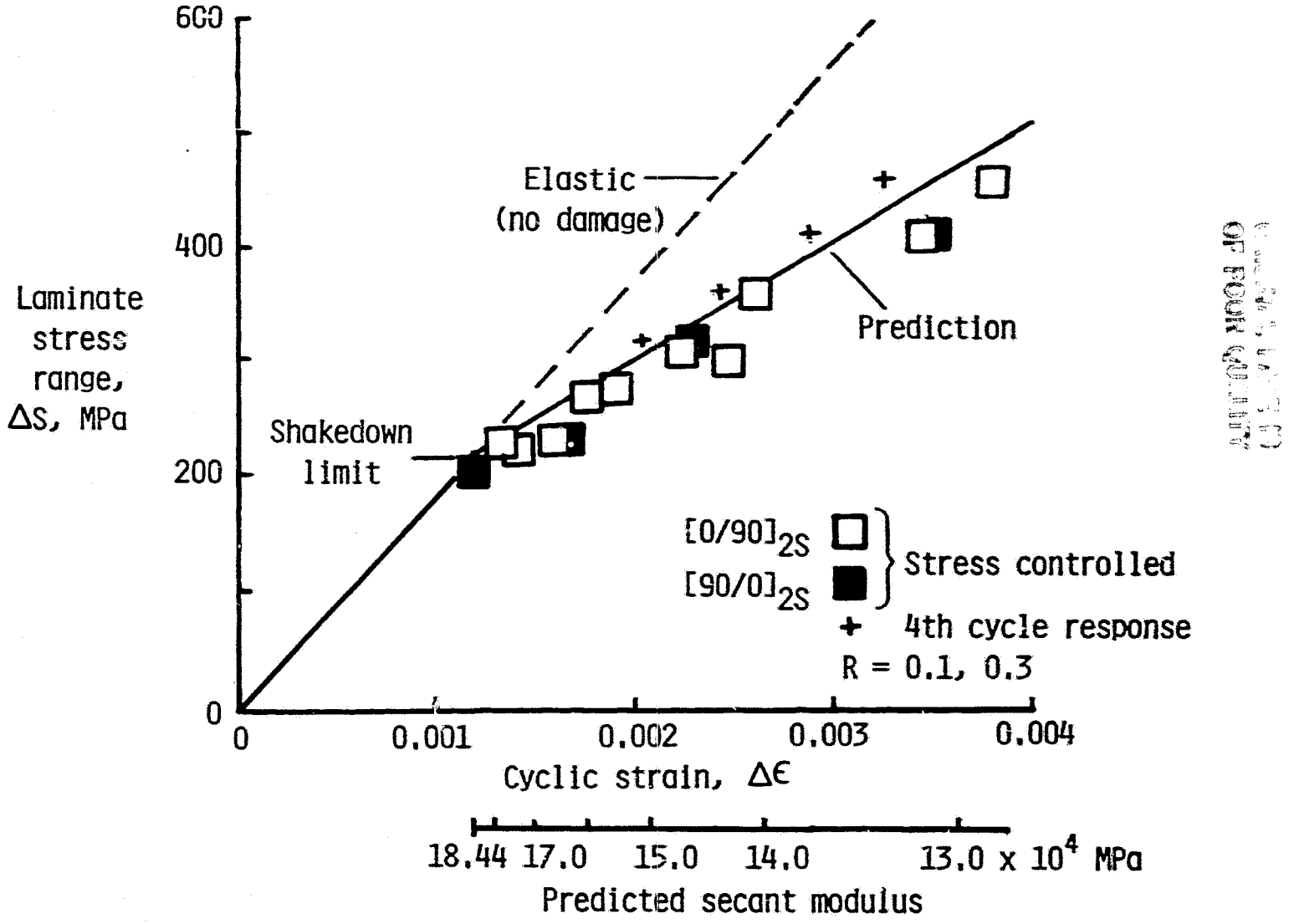

Figure 8.- Correlation of experimental and model predictions for $[0/90]_{2S}$ and $[90/0]_{2S}$ laminates after 500,000 fatigue cycles. The cyclic response for the 4th cycle is shown for some specimens.

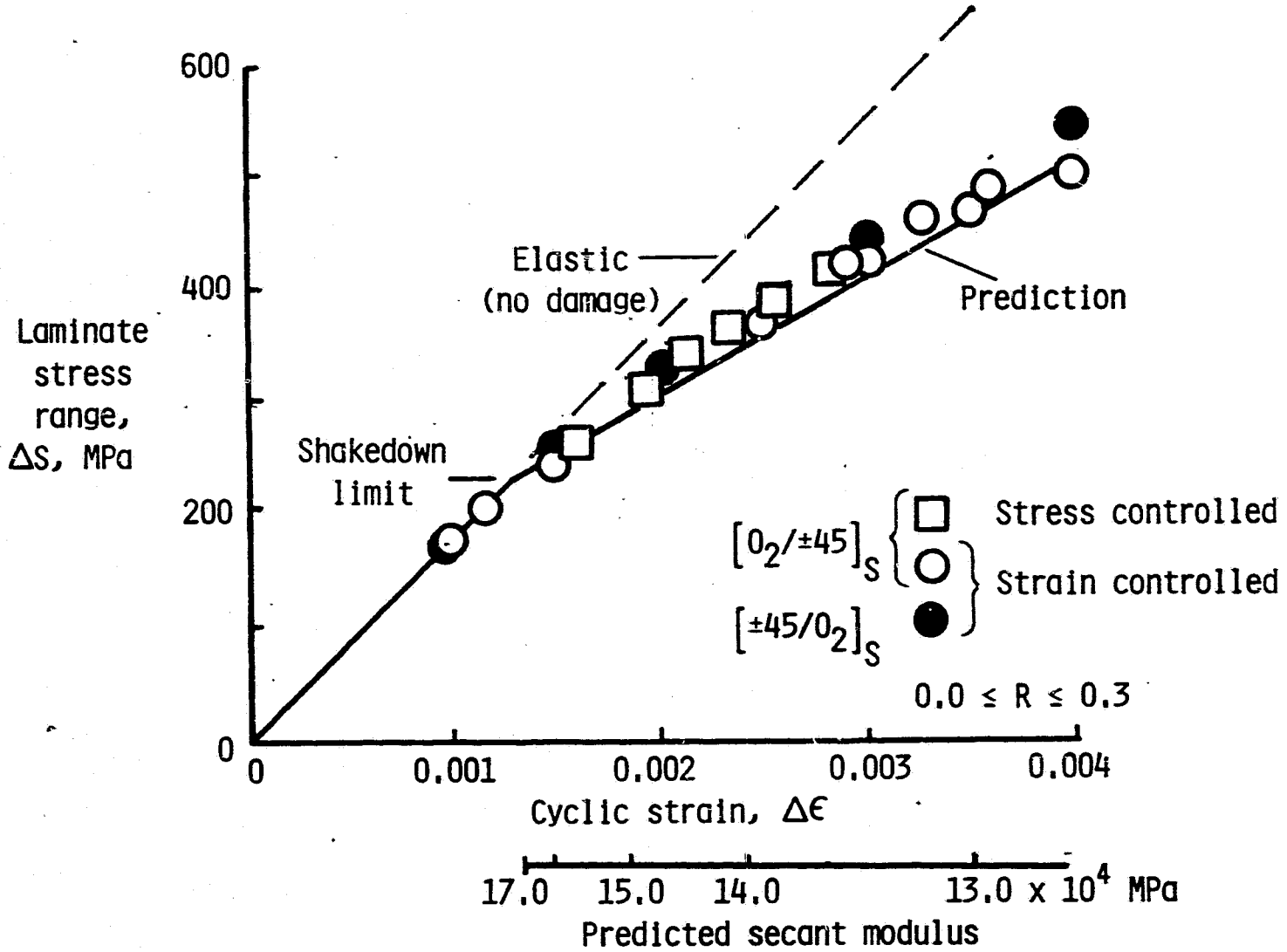

Figure 9.- Correlation between experimental and model predictions for $[0_2/\pm45]_S$ and $[\pm45/0_2]_S$ laminates after 500,000 fatigue cycles.

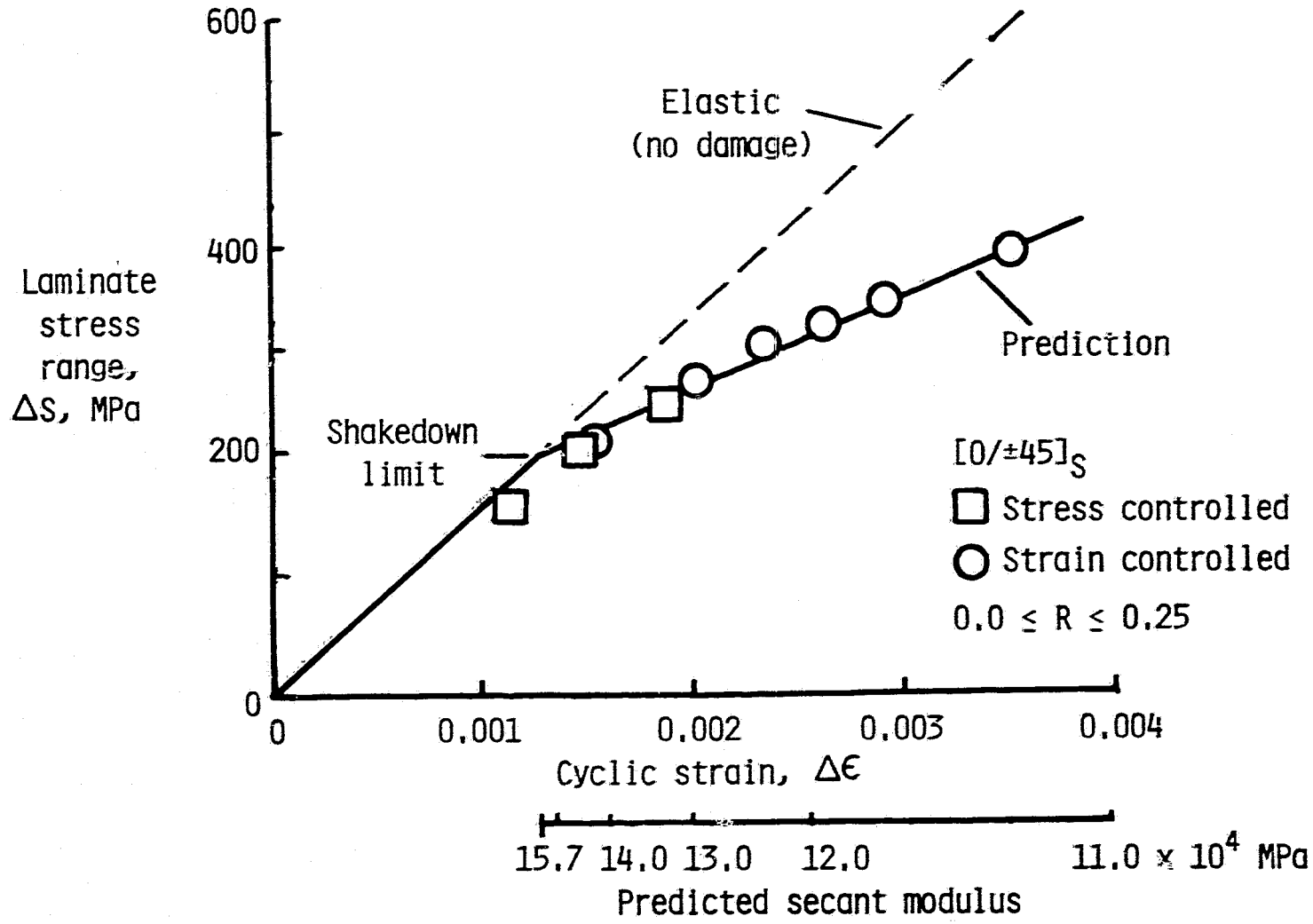

Figure 10.- Correlation between experimental and model predictions for $[0/\pm45]_S$ laminate after 500,000 fatigue cycles.

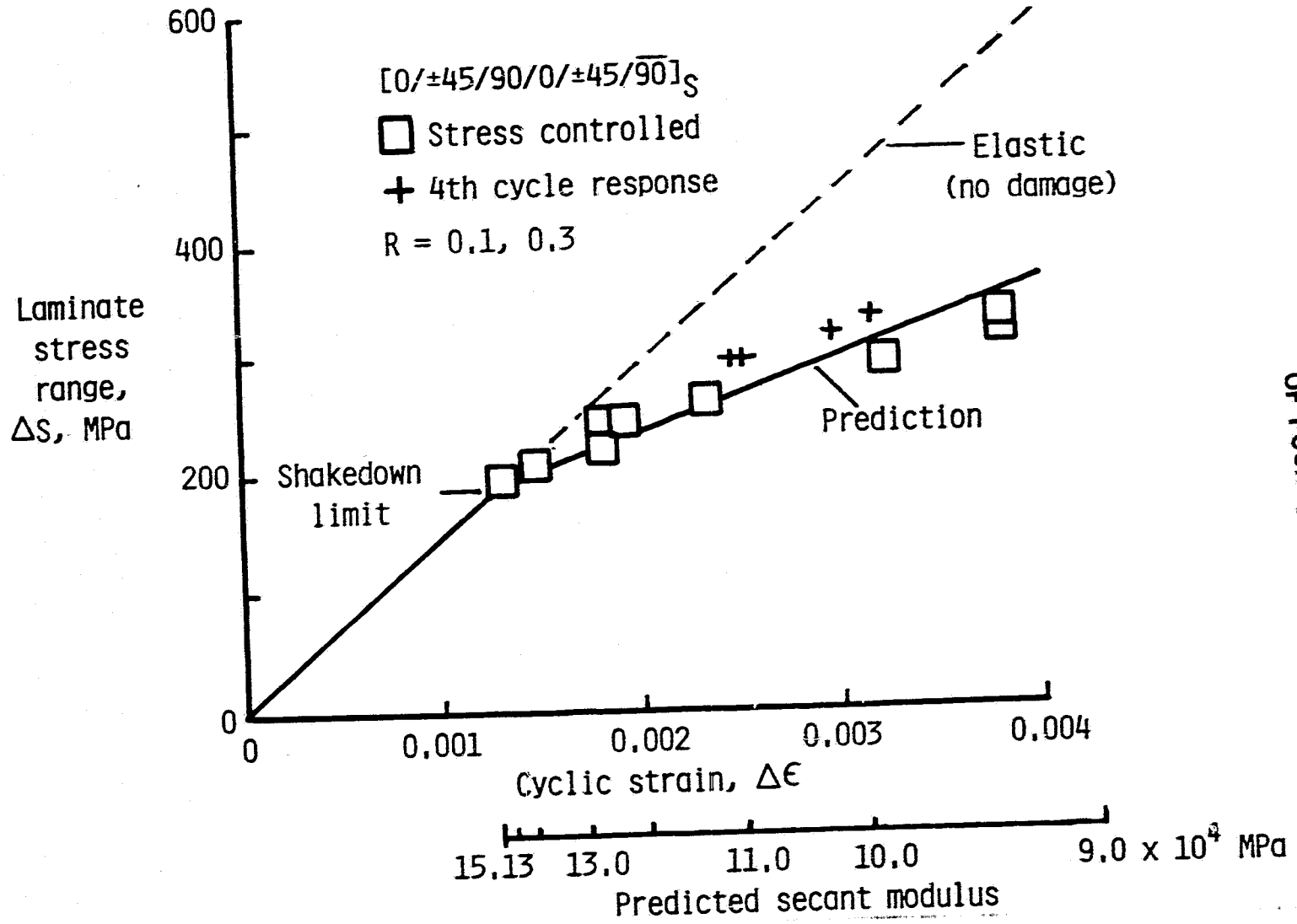

Figure 11.- Correlation between experimental and model predictions for $[0/\pm45/90/0/\pm45/\overline{90}]_S$ laminate after 500,000 fatigue cycles. The cyclic response for the 4th cycle is shown for some specimens.

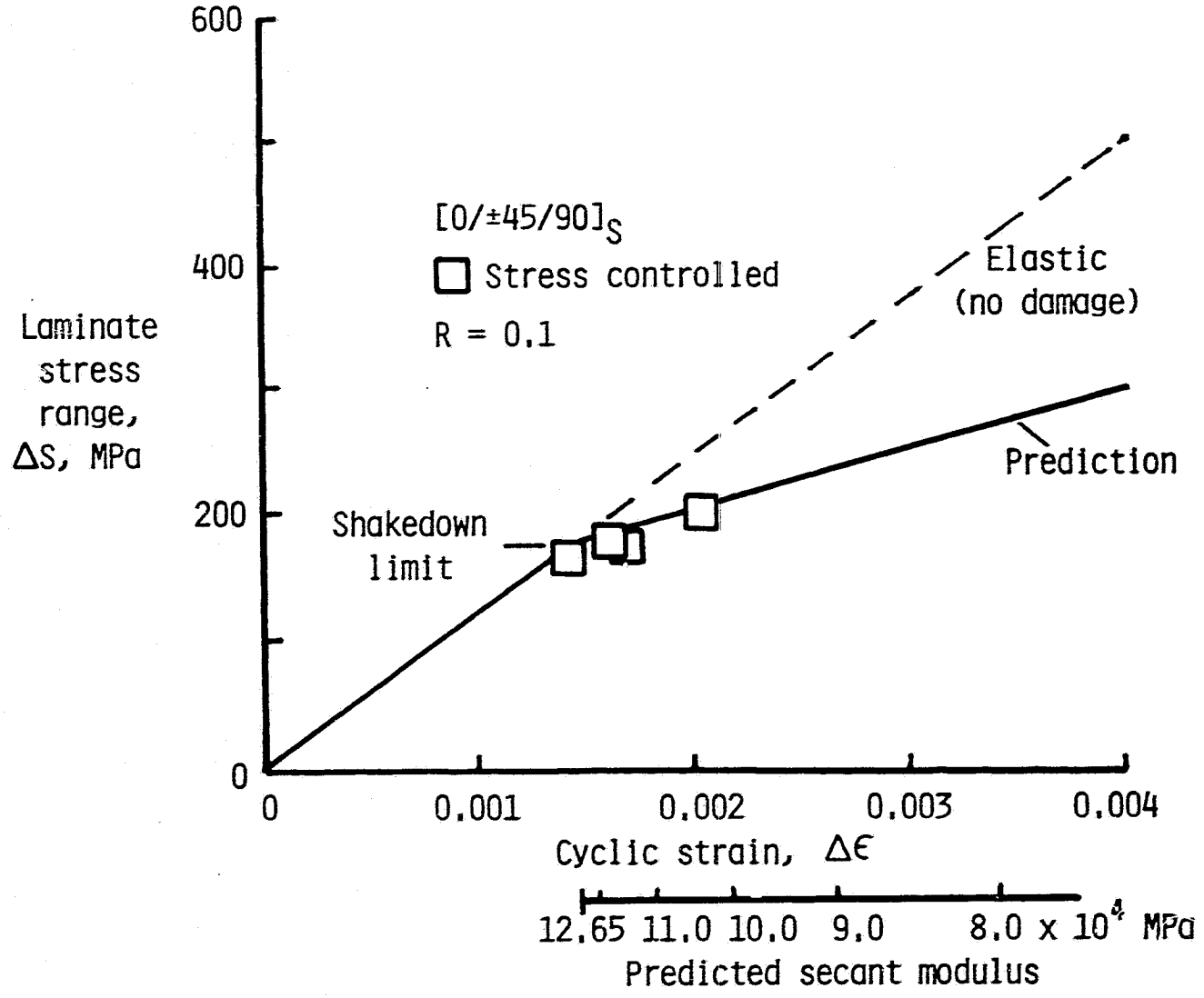

Figure 12.- Correlation between experimental and model predictions for $[0/\pm45/90]_S$ laminate after 500,000 fatigue cycles.